JOURNAL OF SOLID STATE CHEMISTRY 89, 39–59 (1990)

Theoretical Calculation of Bulk Properties of Ionic Crystals from the Cluster Approach: Application to NaF

J. M. RECIO, VÍCTOR LUAÑA, AND L. PUEYO

Departamento de Química Física y Analítica, Facultad de Química, Universidad de Oviedo, 33006 Oviedo, Spain

AND M. BERMEJO

Departamento de Física, Escuela de Minas, Universidad de Oviedo, 33071 Oviedo, Spain

Received March 7, 1990

The Theory of Electronic Separability is applied to the calculation of the ground state total energy and related bulk properties of simple ionic crystals. The work is based on a general equation of this theory that gives the total energy of the crystal in terms of additive energies of conjugate clusters. The cluster additive energy is deducible from standard cluster-in-the-lattice calculations once the effective energy of the cluster is partitioned into net (cluster–*in vacuo*) energy and cluster–lattice interaction energy. In this way, the cluster approach becomes a rigorous theoretical tool to compute crystalline bulk properties. Taking the NaF as an example, this approach is discussed for two different cluster sizes: single-ion cluster and octahedral species like NaF_6^{5-} and FNa_6^{5+}. Given the relevance of the interaction energy, several approaches to this quantity are analyzed in detail, from the unphysical stage of its total neglect (cluster–*in vacuo* calculations) to rigorous formulations involving lattice models which are consistent with the Theory of Electronic Separability. The properties of the NaF crystal analyzed in this work include equilibrium geometry, cohesive energy, elastic constants, and external pressure effects on these quantities.

I. Introduction

The observable properties of solids are usually divided into two broad categories: local and bulk properties. The former include phenomena that are determined by interactions within a few atoms, ions, or molecules in the crystal. Examples are localized excitations, properties of impurities and point defects, and covalency. Bulk properties are determined by interactions involving very many centers or, in the limit, the infinite crystal. Crystal geometry, elastic constants, and the equation of state are bulk properties.

The theoretical interpretation of the crystal properties is made in terms of different theoretical approaches, according to the local or nonlocal character of the property in question. In dealing with local properties, the cluster approximation has received much attention in the past years. In this approximation the properties of interest are deduced from the electronic structure of the cluster, a small group of atoms or ions embedded in the rest of the crystal. A few re-

0022-4596/90 $3.00

cent works will suffice to show the wide interest of this approach: Vail and co-workers computed absorption and emission electronic transitions of pure ionic crystals (*1*), and simulated point defects in NaF and MgO (*2, 3*). Brener and Callaway (*4*) and Janssen and Nieuwpoort (*5*) studied the electronic structure and optical spectrum of NiO. Richardson and Janssen (*6*) analyzed the optical excitation energies of the MnS_4^{6-} cluster in Mn : ZnS. Shashkin and Goddard computed the Jahn–Teller splitting of Cu^{2+} in K_2CuF_3 (*7*). Winter *et al.* (*8*) and Barandiarán and Seijo (*9*) investigated the electronic structure of the Cu^+ impurity in NaCl. Green and Jennison (*10*) computed the interatomic Auger rates for initial $1s$, $2s$, and $2p$ holes in the Na^+ ion in NaF.

Clearly, a single cluster calculation is unsuited to describe the bulk crystal properties that by definition are determined by the infinite crystal. However, the Theory of Electronic Separability (TES) when applied to ionic solids (*11*) tells us how to use the cluster approach to obtain bulk properties in a rigorous manner. The TES gives equations for the total energy of the crystal that involve the additive energy of all those active groups necessary to count all different interactions within the crystal. Such active groups are clusters whose electronic structure can be computed by means of quantum-mechanical methods. The additive energy of a cluster includes the net or intracluster energy plus one-half the interaction energy between the cluster and the rest of the lattice. The cluster approach to the total energy requires then the consideration of two or more clusters in such a way that all relevant crystal interactions are present in the sum of the cluster additive energies. In consequence, a general cluster package may be a rigorous tool to compute crystal total energies if (a) the cluster–lattice interaction is included and (b) the net and interaction components of the cluster energy are explicitly determined.

In simple ionic crystals like binary oxides the necessary partition into conjugate clusters is straightforward since there are only three different types of two-body interactions: cation–cation, cation–anion, and anion–anion. In more complex systems the partition may require a little bit of analysis. In a binary compound like NaF the simplest partition consists in single-ion clusters. The conjugate clusters are simply the Na^+ cation and the F^- anion. This partition gives rise to the Perturbed Ion (PI) method, a TES-consistent scheme recently developed in our laboratory that has given very good resuls in alkali halides and hydrides and in MgO (*12, 13*). The next larger cluster is the diatomic NaF "molecule." The effective energy of this cluster contains all relevant two-body interaction within the NaF crystal. In consequence, it does not need a conjugate cluster to generate the crystal total energy which is just the additive energy of this diatomic cluster. Next, we may consider the conjugate (linear or triangular) triatomic NaF_2^- and FNa_2^+ clusters, and so on. In this work we have examined in detail the conjugate octahedral NaF_6^{5-} and FNa_6^{5+} clusters.

Our previous work on the PI model suggests that in computing the bulk properties of simple ionic crystals the size of the cluster may be less important than the quality of the model used for the cluster–lattice interaction. Accordingly, we have focused the attention in the study of different approximations to this interaction.

First, we discuss the simplest approximation of zero cluster–lattice interaction. This stage gives an unbound crystal since the long-range Coulombic attractions are neglected. Next, we consider two intuitive models of cluster–lattice interaction that may be useful in more complex crystals. The first one is the usual point-charge lattice model that neglects the quantum nature of the lattice ions. The second

model corrects the first one by adding nearest-neighbors lattice repulsions. These repulsion are nonempirically deduced from the cluster calculation in the way proposed by Miyoshi and Kashiwagi (*14*). Finally, we examine two rigorous quantum lattice models (*11, 15*) consistent with the ideas of the TES: the Hartree or Coulomb model and the ab initio Model Potential (MP) lattice model. The Hartree model includes nuclear attraction and exact Coulombic repulsion plus the lattice projection required by the TES to maintain cluster-lattice orthogonality. The ab initio MP lattice model enlarges the Hartree model with a nonlocal lattice exchange operator of the form introduced by Huzinaga and co-workers (*16*).

All these lattice models have been interfaced to a cluster package that solves the Hartree–Fock–Roothaan (HFR) equations for an octahedral cluster over a multicenter basis set of Slater-type orbitals (STO). This package was written by Richardson and co-workers as a tool for computing the electronic structure of transition metal ions in crystals (*17*). It has been modified and systematically tested in our laboratory during the last 10 years. Its final version has given good results for this type of system (*15*).

The investigation reported in this paper confirms that the bulk properties of ionic crystals can be accurately computed by following the rules of the TES and using the cluster approximation. In particular, the present nonempirical calculations of crystal geometry and cohesive energy are as good as those obtained with the electron–gas, pair-potential theory (*18*), or the band structure approach (*19*). The present scheme offers significant theoretical advantages. More noticeable is perhaps the possibility of adapting standard quantum-chemical packages to the immediate calculation of bulk properties of crystals. Consideration of clusters of different size shall give significant information on the nature of the interparticle interactions. Given a general cluster package this research should be readily at hand. In particular, the moderately easy incorporation of many-body effects in the calculation, by enlarging the size of the cluster, shall permit us to analyze the importance of these effects in questions like the pressure–volume behavior of the crystal and the pressure at which polymorphic transitions occur. Furthermore, each single cluster calculation in this scheme may give accurate values for local properties which by definition should be well described by a cluster model. Thus, this new approach should give immediate information on the local or nonlocal character of a crystal property, as well as on the relevance of the cluster–lattice interaction in a particular system.

II. Theory

From the application of the TES to ionic solids (*11*) we briefly recall the following. Our first assumption will be that the crystal under consideration can be partitioned into an active group, in which the self-consistent field (SCF) or configuration interaction (CI) equations are solved, and a collection of frozen groups that enter into the SCF process only through the effective potential and the group projection they exert on the active group. Clearly, this partition can be made in a very large number of ways. For a given partition, the energy terms depending explicitly upon the wave function of the active group A are collected in the effective energy of this group

$$E^A_{\text{eff}} = E^A_{\text{net}} + E^A_{\text{int}}, \tag{1}$$

where E^A_{net} is the net energy of the active group collecting all intragroup interactions, and E^A_{int} is the interaction energy of the active group with all frozen groups of the system. The wave function of the A group is

obtained, in a SCF or CI sense, by minimizing its effective energy. E^A_{eff} is then the energy directly obtained in the cluster-in-the-lattice calculation.

Since the effective energies are not additive, because the sum of the interaction terms would count the interaction energy twice, the additive energy of the active group is introduced through Eq. (2):

$$E^A_{\text{add}} = E^A_{\text{net}} + \frac{1}{2}E^A_{\text{int}}. \tag{2}$$

If a crystal is fully partitioned into a A groups, plus b B groups, etc., the crystal energy becomes:

$$E_{\text{crystal}} = aE^A_{\text{add}} + bE^B_{\text{add}} + cE^C_{\text{add}} + \ldots \tag{3}$$

To relate this equation to the cluster approximation we simply identify each A, B, C, . . . group with a cluster whose electronic structure may be calculated by means of a quantum-chemical package. The important point here is to recall that we have to consider in Eq. (3) a collection of clusters containing all different interactions in the crystal.

For binary compounds like NaF the analysis is particularly easy. We can start by considering single-ion clusters. Eq. (3) becomes

$$E_{\text{crystal}} = N\{E_{\text{add}}(\text{Na}^+) + E_{\text{add}}(\text{F}^-)\} \tag{4}$$

if we deal with a crystal containing N NaF "molecules." We say that the Na^+ and F^- ions are conjugated clusters because taken together in Eq. (4) they include the three different two-body interactions in the NaF crystal. Next, we can consider diatomic clusters. In this simple case, the additive energy of the diatomic NaF cluster incorporates all crystal interactions and we do not need a conjugate cluster, although we could formally write

$$E_{\text{crystal}} = (N/2)\{E_{\text{add}}(\text{NaF}) + E_{\text{add}}(\text{FNa})\} \tag{5}$$

if we consider the FNa molecule as the conjugate cluster of the NaF. Since these two conjugate clusters are the same system, the energy of the crystal per molecule is just the additive energy of the NaF cluster. The difference between Eqs. (4) and (5) is that a two-center electron density is created in the SCF solution of the latter. This incorporates further variational freedom as well as a SCF treatment for the two-center interactions. In the same way we can write for triatomic clusters

$$E_{\text{crystal}} = (N/3)\{E_{\text{add}}(\text{NaF}_2^-) + E_{\text{add}}(\text{FNa}_2^+)\} \tag{6}$$

and for octahedral clusters

$$E_{\text{crystal}} = (N/7)\{E_{\text{add}}(\text{NaF}_6^{5-}) + E_{\text{add}}(\text{FNa}_6^{5+})\}. \tag{7}$$

Thus, more accurate description of the multicenter interactions and increasing variational freedom are gained when the size of the cluster increases. The price is obviously the need for more sophisticated computer programs and greater amounts of computer time.

The ideal application of formulas like Eqs. (6) and (7) involves accurate cluster calculations and rigorous models for the cluster–lattice interaction appearing in the effective and additive energies. The cluster calculation demands an all electron Hartree–Fock calculation plus a detailed consideration of the electron correlation. The cluster–lattice interaction demands mathematical and physical consistency between cluster and lattice models, which means accurate wave functions to describe the lattice atoms or ions, accurate coulomb and exchange interaction between cluster and lattice electrons, plus a mathematical device to interface the cluster and lattice descriptions. However, one frequently has to introduce approximations in the cluster calculation (core-valence partition, integral approximations, small basis sets if the Roothaan

scheme is adopted, lack or insufficient amount of electron correlation, etc.) as well as in the lattice model (use of a point-charge lattice, free-space effective potentials, lack or insufficient cluster–lattice interfacing, etc.). The introduction of approximations makes it necessary to analyze how well a given model can work, i.e., how much accurate information and how many physical ideas can be obtained from it. This type of analysis is reported in the following sections. We present here several applications of Eq. (7) as well as a very brief comment on Eq. (4).

III. Single-Ion Clusters: The Perturbed Ion Method

We will not discuss this stage because the Perturbed Ion (PI) method has been recently reported, with particular reference to NaF and other alkali halides and hydrides (*12, 13*). We simply will recall that, whereas the PI atomic-like orbitals for the Na^+ ion are very close to the free ion AOs, the fluoride $2p$ PI AO shows a noticeable contraction with respect to the free ion orbital. This anionic contraction makes the crystal stable. The ground state total energy shows a minimum at 2.371 Å, 0.054 Å larger than the experimental value. The cohesive energy at this geometry is 218.7 kcal/mole, to be compared with experimental values ranging from 214 to 221 kcal/mole. The bulk modulus given by the PI calculation is 49.1 GPa, the experimental data ranging from 46.5 to 51.5 GPa. The pressure derivatives of this modulus and the pressure dependence of the cell volume also agree with available experimental data.

The PI model is fully consistent with the TES. Its implementation gives an efficient algorithm to compute the bulk properties of the alkali halides. The use of Eq. (4) makes the complete PI calculation very economic. Moreover, the PI model works also as a basis set generator. It produces atomic-like orbitals that are consistent with the (quantum-mechanically described) crystalline environment. On the other hand, it is the first step in an accurate cluster calculation. All multicenter interactions are neglected in the PI SCF process, with the corresponding loss of physical detail and variational freedom.

IV. Octahedral Clusters: Simple Lattice Models

We now report results obtained from Eq. (7). Three intuitive models for the cluster–lattice interaction (including its total neglect) have been considered, as follows.

A. Total Neglect of the Cluster–Lattice Interaction

This stage corresponds to the cluster–*in vacuo* description. The classical, point-charge approximation gives a cluster net energy of the form

$$E_{\text{class}}(R) = 6q_M q_L/R + [6(2)^{1/2} + 3/2]q_L^2/R, \tag{8}$$

where q_M and q_L are point-charges representing the metal and ligand ions separated a distance R in the octahedral cluster. $E_{\text{class}}(R)$ is a continuously repulsive curve that gives a bound cluster state when the cluster–lattice interaction is added to it (*20*).

To describe these systems quantum-mechanically, we have used the original HFR programs for octahedral clusters developed by Richardson's group (*17*). Given the highly ionic character of the NaF crystal, the renormalization correction (*21, 22*) and the core projection (*23, 24*) have been neglected at this stage.

New reduced basis sets for Na^+ and F^- ions have been generated for the present calculation. The Na^+ basis was prepared as follows. First, the Clementi–Roetti (*25*) multi-ζ basis is reduced to a $3s2p$ size by means of the maximum-overlap algorithm of Francisco *et al.* (*26*). Then the atomic

TABLE I

PSEUDO-HARTREE–FOCK BASIS SETS PREPARED IN THIS WORK (B2 BASIS) FOR Na^+ AND F^- IONS

n	ζ	$1s$	$2s$	n	ζ	$2p$
			F^-			
1	8.57204	0.9969828	−.2581086	2	3.26799	0.5728137
2	2.86217	0.0122767	0.7748277	2	1.26842	0.5512582
2	1.62753	−.0044244	0.2948616	$\varepsilon(nl)$		−0.17894
$\varepsilon(nl)$		−25.88860	−1.07306			
			Na^+			
1	10.54139	0.9969036	−.2789483	2	5.04838	0.4117595
2	3.50197	0.0133373	0.9016370	2	2.43709	0.6609965
2	2.14034	−.0054706	0.1527821	$\varepsilon(nl)$		−1.79855
$\varepsilon(nl)$		−40.75815	−3.05504			

SCF program is executed over the reduced set of orbital exponents. This gives the final basis. The F^- ion has been described with two different basis. The first one is the minimal basis reported in Ref. (*27*). This choice plus the new set for the Na^+ ion will form the B1 basis from now on. The second fluoride basis has been prepared from Clementi–Roetti sets in the manner described for the Na^+ ion. This $3s2p$ choice plus the Na^+ basis form the B2 basis. The new B2 set can be seen in Table I.

The HFR equations have been solved for the NaF_6^{5-} and FNa_6^{5+} clusters *in vacuo*, within the B1 and B2 bases, at several values of R. At this stage, the net energy of the cluster coincides with the additive and effective energies. The net energy is collected in Table II. Equation (7) gives us the energy of the crystal, also appearing in the table. As expected, all these calculations give repulsive clusters (see the curves at the top of Fig. 1) and an unbound crystal for the range $4 \leq R \leq 5$ bohr (see Fig. 2A). Use of small

TABLE II

CLUSTER ADDITIVE ENERGY AND CRYSTAL ENERGY FROM B1 AND B2 CLUSTER–*IN VACUO* CALCULATIONS

R(Å)	$E_{add}[NaF_6^{5-}]$	$E_{add}[Fna_6^{5+}]$	$E_{crystal}$
		B1 basis	
2.15	−752.65704	−1067.21266	−259.98139
2.25	−752.71198	−1067.26728	−259.99704
2.35	−752.75832	−1067.31345	−260.01025
2.45	−752.79858	−1067.35363	−260.02174
2.60	−752.85005	−1067.40506	−260.03644
∞	−753.66352	−1068.21839	−260.26885
		B2 basis	
2.15	−756.62643	−1067.81160	−260.63543
2.25	−756.71237	−1067.88643	−260.65697
2.35	−756.77450	−1067.94793	−260.67463
2.45	−756.82656	−1067.99961	−260.68945
2.60	−756.89005	−1068.06277	−260.70755
∞	−757.72267	−1068.89492	−260.94537

basis sets and neglecting the cluster–lattice interaction are responsible for this repulsive energy curves. Basis sets enlarged with diffuse functions can give, at the cluster–*in vacuo* level, a cluster effective energy curve with a shallow minimum for the ground state of the NaF_6^{5-} cluster, as discussed by Bermejo *et al.* (*28*). The cluster–lattice interaction can also produce such minima, as we show below.

From Table II we can observe that the difference $E_{net}(R) - E_{net}(\infty)$ is nearly the same for the two clusters in the B1 calculation. This small basis makes the clusters slightly more repulsive than the classical one. The B2 calculation gives still more repulsive clusters because the fluoride orbitals are more diffuse in this representation. We can also notice the variational improvement associated with the larger B2 basis.

This calculation is thus totally inadequate to obtain bulk properties of the crystal. Before passing to the next level of approximation, we will obtain the nonclassical intracluster interaction energy by subtracting the classical term in Eq. (8) from the difference $E_{net}(R) - E_{net}(\infty)$. If we further assume that the nonclassical fluoride–fluoride interaction is negligible, we have the following nonclassical, sodium–fluoride pair energy:

$$E_{nc}(R) = \frac{1}{6}([E_{net}(R) - E_{net}(\infty)] - E_{class}(R)). \tag{9}$$

The assumption of zero nonclassical F^-–F^- energy is consistent with the neglect of the renormalization correction in the quantum calculation. It seems also reasonable in view of the quasi-classical behavior of the fluoride ion in the HFR calculation. The first-principles $E_{nc}(R)$ in Eq. (9) will be incorporated later on in the cluster–lattice interaction as a short-range repulsion, in the manner proposed by Miyoshi and Kashiwagi (*14*). The resulting values of $E_{nc}(R)$ can

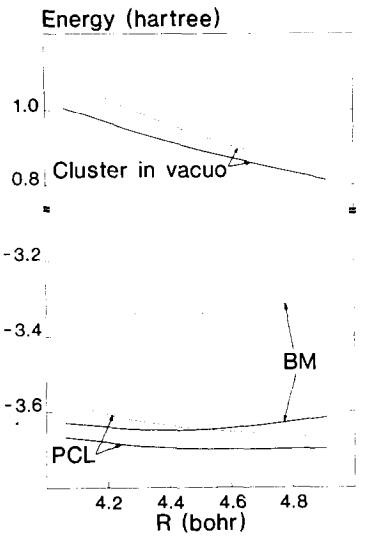

FIG. 1. B1 (solid lines) and B2 (dotted) cluster effective energy, referred to $E_{eff}(\infty)$, for the FNa_6^{5+} system *in vacuo* and embedded into a fixed, point-charge lattice (PCL), and a Born–Mayer (BM) lattice.

be very well represented by simple exponential expressions of the Born–Mayer type (in atomic units):

$$E_{nc}^{B1}(R) = 1139.957 \exp(-3.08688\,R) \tag{10}$$

$$E_{nc}^{B2}(R) = 26.23721 \exp(-1.80971\,R). \tag{11}$$

Notice that the more compact B1 basis gives a sharper repulsion.

B. The Point-Charge Lattice

First, let us recall that in dealing with octahedral clusters and a nonvanishing cluster–lattice interaction, the ground state equilibrium geometry of a crystal like NaF can be obtained from three different energy curves: (a) the $E_{eff}(R)$ curve of the NaF_6^{5-} cluster in a fixed lattice, (b) the $E_{eff}(R)$ curve of the FNa_6^{5+} cluster in a fixed lattice, and (c) the $E_{crystal}(R)$ curve, Eq. (7). In the last case, a different lattice parameter is used for each different cluster-in-the-lattice calculation, i.e., the vertical calculation of E_{add} (NaF_6^{5-}) and $E_{add}(FNa_6^{5+})$ at a Na^+–F^- dis-

tance R_i involves a lattice with first-neighbors distance equal to R_i.

In the point-charge lattice model we compute the lattice potential by means of the Ewald method at very many points within the cluster volume. These numerical values are then represented by an accurate one-particle fitting function in the manner described in Ref. (*11*). This function is included in the cluster Fock operator before the convergence process.

The ground state effective energy of the FNa_6^{5+} cluster, as obtained with the point-charge lattice fixed at the observed geometry, is plotted in Fig. 1. The coulombic attraction is strong enough to produce a minimum in the B1 curve. The cluster repulsions within the B2 basis are larger than this lattice attraction and the B2 curve gives an unbound cluster.

The results of the crystal calculation in terms of Eq. (7) appear in Table III. Figure 2B shows that both bases give unstable crystals at this level of approximation. B1 basis gives a crystal energy slightly different from the Madelung value. B2 basis shows again a larger repulsion. Both calculations tell us that the lattice attractions surpass the intracluster repulsions. The result is a collapsing crystal.

C. The Born–Mayer Lattice

Finally, let us see results from cluster-in-the-lattice calculations involving short-range repulsions of the Born–Mayer type. These repulsions have been added to the interaction energy as a perturbation, after the SCF process. As noted before, only metal–fluoride repulsions have been considered, through Eqs. (10), and (11).

The effective energy of the FNa_6^{5+} cluster in the experimental lattice can be seen in Fig. 1. Both bases give a bound cluster. Notice that these nonempirical Born–Mayer repulsions depend upon the basis set used in the cluster calculation. B2 repulsions are noticeably larger than the B1 values.

The crystal calculations are collected in Table IV and the crystal energy, referred to the infinitely separated ions, has been plotted in Fig. 2C. The small B1 repulsion deviates the crystal energy from the Madelung value only at the shorter distances. The B2 basis, with a larger repulsion that increases at shorter distances, gives a bound crystal. From this ground state curve we obtain R_e = 2.369 Å (2.317 Å experimental) and a cohesive energy of 213.5 kcal/mole.

Notice, finally, the two remarkably different predictions obtained in this section: (a) the geometry of a cluster embedded in the observed lattice (Fig. 1), using the cluster effective energy, and (b) the geometry of the crystal, from Eq. (7). The second prediction means that the simple point-charge lattice model is still unsuited to obtain bulk properties of the crystal, although the local properties associated to the cluster may be evaluated at this level with the B1 basis. Of course, in this pure system the crystal and the cluster are the same chemical species and the above difference is unphysical. In an impurity system, like $Cr^+ : NaF$, the difference makes sense. The present analysis shows the different meaning of these two calculations, the more economic approach to the local or cluster properties, and the possibility of obtaining bulk properties from the cluster approximation and Eq. (7).

A few words of caution should be added here. The lattice repulsion correction introduced in the manner proposed in Ref. (*14*) makes use of the next-neighbor position to estimate the repulsion energy. This necessarily must lead to a bound cluster unless a poorly flexible basis should give rise to a very small lattice correction. Indeed, we could argue that the value of R_e obtained in the calculation is already present in the algorithm through this correction. Thus, not too much meaning must be attached to the apparently successful result of this approach. Only when the lattice interactions are introduced in a completely nonempirical

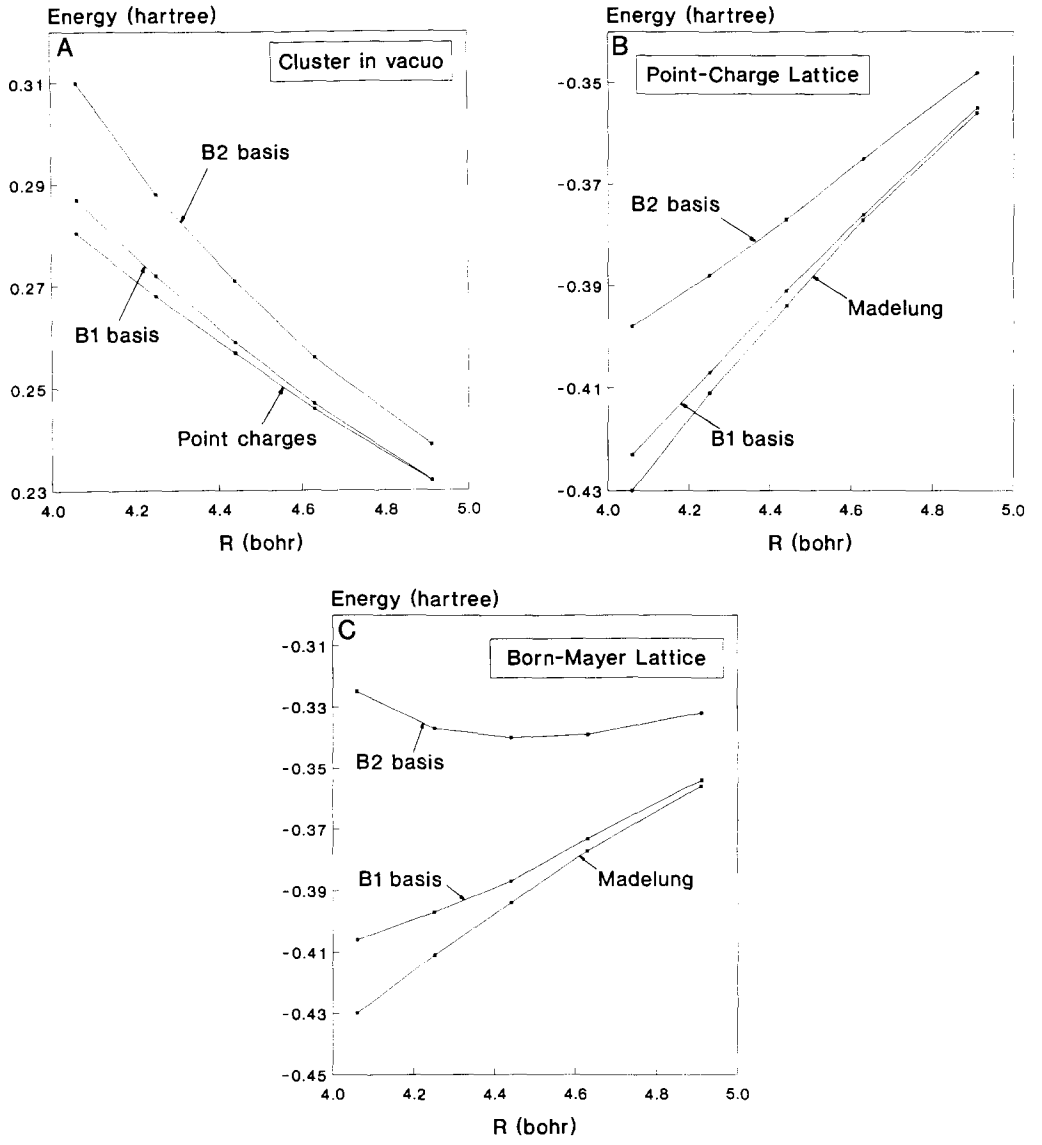

FIG. 2. Crystal energy of NaF referred to the infinitely separated ions (Eq. (7)).

manner can we use the resulting values of the geometrical parameters as a guide to appraise the performance of the calculation.

From the $E_{\text{crystal}}(R)$ curve obtained in the Born–Mayer–B2 calculation we can deduce elastic constants and the high-pressure behavior of the crystal. The three independent elastic constants of the cubic crystal can be partitioned into pure-electrostatic and short-range contributions (*18*). The classical terms were given by Cowley (*29*). The short-range contribution depends upon the form of the potential. For nearest-neighbors potentials the expressions are (*18*):

$$C_{11}^{\text{SR}} = (1/R)(d^2V(+,-)/dR^2)_0 \qquad (12)$$

TABLE III

RESULTS FROM THE POINT-CHARGE LATTICE MODEL

R(Å)	$E_{add}[NaF_6^{5-}]$	$E_{add}[Fna_6^{5+}]$	$E_{crystal}$
		B1 basis	
2.15	−755.14515	−1069.70077	−260.69227
2.25	−755.08886	−1069.64416	−260.67615
2.35	−755.03349	−1069.58862	−260.66030
2.45	−754.98038	−1069.53543	−260.64512
2.60	−754.90743	−1069.46244	−260.62427
∞	−753.66352	−1068.21839	−260.26885
		B2 basis	
2.15	−759.10422	−1070.29639	−261.34294
2.25	−759.07939	−1070.25345	−261.33326
2.35	−759.04023	−1070.21366	−261.32198
2.45	−758.99931	−1070.17236	−261.31024
2.60	−758.93890	−1070.11162	−261.29293
∞	−757.72267	−1068.89492	−260.94537

$$C_{12}^{SR} = -(1/R^2)(dV(+,-)/dR)_0 \quad (13)$$

$$C_{44}^{SR} = (1/R^2)(dV(+,-)/dR)_0 \quad (14)$$

where SR is short-range contribution, $V(+,-)$ is the nearest-neighbors short-range potential, and the subscript 0 indicates that the derivatives must be evaluated at the equilibrium geometry. Using Eq. (11) for $V(+,-)$ we find

$$C_{11} = -1.27802/a^4 + A\sigma^2\exp(-\sigma a)/a \quad (15)$$

$$C_{12} = 0.05649/a^4 + A\sigma\exp(-\sigma a)/a^2 \quad (16)$$

$$C_{44} = 0.63901/a^4 - A\sigma\exp(-\sigma a)/a^2 \quad (17)$$

with $A = 26.23721$ and $\sigma = 1.80971$. The bulk modulus is given by

TABLE IV

RESULTS FROM THE BORN–MAYER LATTICE MODEL

R(Å)	$E_{add}[NaF_6^{5-}]$	$E_{add}[Fna_6^{5+}]$	$E_{crystal}$
		B1 basis	
2.15	−755.08348	−1069.63910	−260.67465
2.25	−755.05456	−1069.60986	−260.66634
2.35	−755.01756	−1069.57269	−260.65575
2.45	−754.96977	−1069.52482	−260.64208
2.60	−754.90296	−1069.45797	−260.62299
∞	−753.66352	−1068.21839	−260.26885
		B2 basis	
2.15	−758.85067	−1070.04284	−261.27050
2.25	−758.89962	−1070.07368	−261.28190
2.35	−758.91276	−1070.08619	−261.28556
2.45	−758.90893	−1070.08198	−261.28442
2.60	−758.88445	−1070.05717	−261.27737
∞	−757.72267	−1068.89492	−260.94537

TABLE V

EQUILIBRIUM GEOMETRY (Å), BINDING ENERGY (kcal/mole), ELASTIC CONSTANTS (GPa), AND fcc–bcc TRANSITION PRESSURE (GPa)

Ref.	R_e	E_0	C_{11}	C_{12}	C_{44}	B	C'	p
(*26*)	2.29	205.1		25.19	31.63	27.03		
(*18*)	2.305	211.9	80.0	27.8	27.8	45.5	26.5	32.6
(*40*)	2.241	202.4				55.8		<0
(*19*)	2.317	224.7				64.9		
(*39*)	2.283	223				50.8		20.0
This work	2.369	213.5	77.2	25.2	25.7	42.5	25.9	
Experimental	2.295[a]	216.0[b]	108.5[c]	22.9[c]	29.0[c]	51.4[c]	42.8[c]	27[d]

[a] Ref. (*42*).
[b] Ref. (*43*).
[c] Ref. (*37*).
[d] Ref. (*31*).

$$B = (C_{11} + 2C_{12})/3 \quad (18)$$

and the shear modulus by

$$C' = (C_{11} - C_{12})/2. \quad (19)$$

The results of this calculation are collected in Table V. The predictions of this simple model are reasonably accurate and compare well with those obtained by Cohen and Gordon (*18*) and other workers. The equilibrium distance is 0.05 Å larger than the experimental value but the cohesive energy deviates only by 2.5 kcal/mole. The elastic constants are similar to those reported in Ref. (*18*). Notice that the experimental values have been obtained at 4.3 K, where zero-point effects may be significant. Our computed C_{12} is slightly larger than C_{44}, in agreement with the experimental ordering. This deviation from the Cauchy relation ($C_{12} = C_{44} + 2p$, p being the external pressure) may be attributed to the small multicenter energy terms appearing in the intracluster part of our crystal calculation, since the Cauchy relation holds in centrosymmetric crystals with two-body interionic potentials. The small difference between our values for C_{44} and C' is also consistent with the observed trends in alkali halides.

To end this section we will discuss briefly the predictions of this model on the pressure behavior of the elastic constants of the NaF. The Gibbs free energy of the crystal at 0 K can be written as a function of the external pressure and the interionic distance

$$G(R, p) = E_{\text{crystal}}(R) + 2p\,R^3, \quad (20)$$

since the "molecular" volume of the fcc phase is $2R^3$. Taking the crystal energy, computed with the B2 basis, into Eq. (20) we find the free-energy isobars of Fig. 3. We see that the Gibbs function increases and

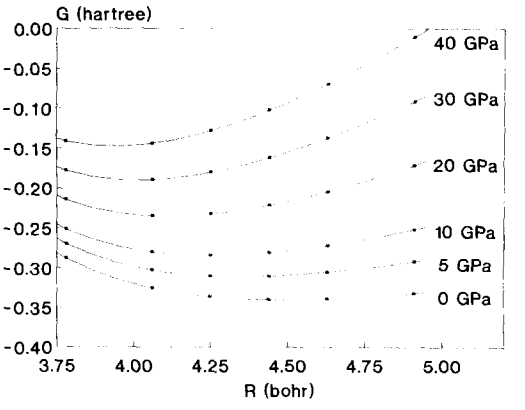

FIG. 3. Gibbs free-energy isobars (hartree), Eq. (20), as computed from the BM–B2 model.

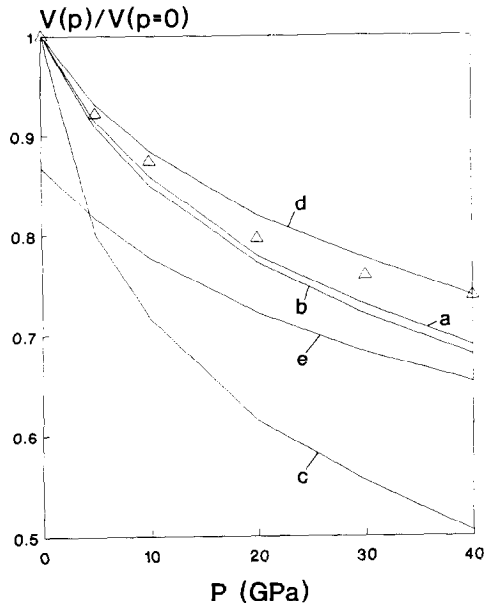

FIG. 4. Pressure–volume diagram for the NaF crystal: (a) Ref. (*18*); (b) BM–B2 calculation: (c) Ref. (*19*); (d) MP fcc; (e) MP bcc. Open triangles are experimental data from Ref. (*30*).

the interionic distance decreases when the pressure increases, as it should be. The curvature of these isobars at the minimum also increases with increasing pressure, in agreement with the known pressure dependence of the bulk modulus.

The minima of the isobars give the equilibrium geometry as a function of the external pressure, i.e., the p–V behavior of the crystal. This information is plotted in Fig. 4 with the experimental results obtained by Drickamer *et al.* (*30*). Our results are very close to those by Cohen and Gordon (*18*) and follow rather well the observed trend. Deviations from experiment increase with pressure but they are, in the worse case, smaller than 8%.

The pressure behavior of the elastic constants has been computed by introducing the equilibrium distance of each isobar into Eqs. (15–19). This gives the numbers in Table VI. The linear dependence of C_{11}, C_{12}, C_{44}, and B with the applied pressure can be clearly seen in Fig. 5. Our deviation from the Cauchy relation increases smoothly with increasing pressure, as expected. It is, in any case, smaller than 10%. C_{44} decreases with increasing pressure and nearly vanishes at 50 GPa. Such pressure gives the stability limit for this phase, i.e., any phase transition should appear at smaller pressures. Cohen and Gordon predicted a fcc–bcc transition at 32.6 GPa (*18*). Yagi, Suzuki, and Akimoto (*31*) reported such transition at 27 GPa with a volume change at the transition of -8.9%. On the other hand, Drickamer data indicate that the fcc phase is the more stable one up to 40 GPa.

The comparison of the plots in Fig. 5 with the experiment is not easy since the measurements go up to a few gigapascals. Roberts and Smith (*32*) and Hart and Greenwood (*33, 34*) give the pressure derivatives at zero pressure for the C_{ij}. The first derivative is largest for C_{11} and nearly zero for C_{44}. The second derivative is very small for these three constants and positive only for C_{12}. Our results in Fig. 5 are qualitatively consistent with these observations although the observed variation of the C_{ij} with pressure is larger than that deduced from our model. A very similar discrepancy is found in the theoretical results by Cohen and Gordon (*18*).

The performance of the simple model discussed in this section is qualitatively correct and quantitatively rather accurate. Those properties determined by the first derivative of the crystal energy curve are computed in better agreement with the experiment than those related to the second derivative, which are more sensitive to contributions from nonclassical energy terms between equal ions. Such interactions have been neglected in this work beyond the intracluster calculation. The computed elastic constants, their pressure behavior, and the p–V diagram obtained here show a crystal softer than the real one. This is clearly a consequence of neglecting the very many short-

TABLE VI

PRESSURE DEPENDENCE OF THE EQUILIBRIUM INTERIONIC DISTANCE (Å) AND THE ELASTIC CONSTANTS (GPa)

p(GPa)	R_e	C_{11}	C_{12}	C_{44}	B	C'	$C_{44} + 2p$
0	2.370	77.2	25.2	25.7	42.5	25.9	25.7
10	2.246	159.2	40.9	22.1	80.4	59.1	42.1
20	2.175	229.6	54.4	17.3	112.8	87.6	57.3
30	2.125	295.4	67.0	11.8	143.1	114.2	71.8
40	2.085	357.6	78.9	6.0	171.8	139.3	86.0
50	2.052	418.6	90.7	−0.2	200.0	163.1	99.8

Note. Last column has been added to see the deviation from the Cauchy relation ($C_{12} = C_{44} + 2p$).

range repulsions in the cluster–lattice interaction, although some error may be introduced by the simple formula adopted to estimate the repulsions from the intracluster energy.

This model should be viewed as a straightforward extension of the entirely classical model described in Ref. (*20*), where inter- and intracluster interactions were approximated by point-charge potentials. The quantum correction introduced here eliminates in part the empirical character of this crude approach, at least in the treatment of the short-range terms.

V. Octahedral Clusters: Rigorous Lattice Models

The work reported in this section has been performed with the B2 basis. Intracluster interactions have been computed more accurately because the renormalization correction (*21, 22*) and the core projection (*13, 14*) have been considered. The first correction improves the description of the ligand–ligand interactions by computing a collection of integrals neglected at the unrenormalized stage. The second one nearly eliminates the unwanted two-center, core-valence nonorthogonality introduced by the frozen-core approximation. These two corrections increase the total intracluster electron repulsion at short distances and tend to vanish when R increases.

The two lattice models discussed in this section have been described in Ref. (*15*). Here we will give only the necessary details. The lattice ions are now explicitly considered as quantum-mechanical species. They are described with the B2 basis in Table I.

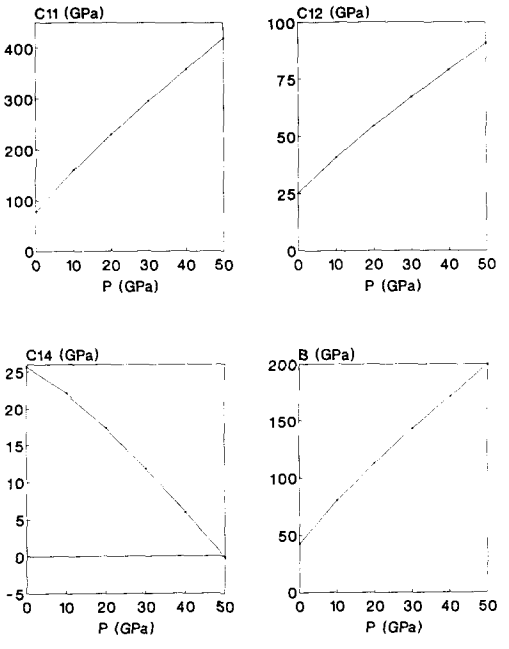

FIG. 5. Pressure dependence of the elastic constants (GPa) of the NaF.

At the i^{th} point of the cluster the S lattice ion produces an effective potential of the form

$$V^S_{\text{eff}}(i) = -Z^S r_{iS}^{-1} + V^S_C(i) + V^S_X(i), \quad (21)$$

where Z^S is the nuclear charge,

$$V^S_C(i) = \int \rho^S(r_2) r_{12}^{-1} d\tau_2 \quad (22)$$

is the Coulombic electron repulsion, and

$$V^S_X(i) = -\sum_l \sum_{m=-l}^{+l} \sum_{a,b} | alm,S> A(l,a,b,S) <blm,S | \quad (23)$$

is a nonlocal exchange approximation introduced by Huzinaga *et al.* (*16*) and incorporated in solid state calculations by Barandiarán and Seijo (*9*).

In Eq. (23), $\{ | alm,S> \}$ are products of spherical harmonics and primitive radial functions for the S ion. The $A(l,ab,S)$ numbers are the elements of the matrix

$$\boldsymbol{A} = \boldsymbol{S}^{-1} \boldsymbol{K} \boldsymbol{S}^{-1} \quad (24)$$

and $\boldsymbol{S}$ and $\boldsymbol{K}$ are the overlap and exchange matrices for the S ion in the $\{ | alm,S> \}$ basis.

The lattice effective potential V_{eff} is the sum of the ionic potentials V^S_{eff} for all ions in the lattice. The lattice effective Hamiltonian is made of V_{eff} and the lattice projection operator

$$P^S(i) = \sum_{g \in S} | \psi^S_g > (\kappa_g) < \psi^S_g | , \quad (25)$$

where g runs over all occupied orbitals ψ^S_g. The projection constants κ_g have been identified here with the negative of the orbital energy of the ψ_g orbital. These energies have been collected in Table I.

The effective lattice potential and the lattice projector decay rather quickly with increasing distance. We have seen that only the 50 ions in the first four layers around the reference cluster give nonvanishing contributions to the quantum lattice operators. This permits us to partition computationally the crystal into a quantum and a classical lattice. The first one is made of the 50 ions separated a distance R_i from the center of the cluster with $2^{1/2}R_0 \leq R_i \leq 5^{1/2}R_0$, R_0 being the smallest interionic distance in the lattice. The remaining ions form the classical lattice and may be considered as point charges. Thus, they contribute nothing to the lattice projector and give a lattice potential that is computed through the Ewald method as discussed before.

TABLE VII

OPTIMUM PARAMETERS FOR THE MODEL POTENTIAL IN EQ. (26), *B2* BASIS

$n(k,S)$	$A(k,S)$	$\alpha(k,S)$
	Na^+ $Z = 11$ $N = 3$	
0	10.053 495 631	1.494 920 816
1	−12.749 541 568	1.964 747 574
1	−15.428 454 108	12.511 007 976
	F^- $Z = 9$ $N = 3$	
0	−10.044 679 758	1.979 006 678
1	−0.063 634 592	0.962 386 798
1	13.227 511 685	9.194 318 964

The sum of nuclear attraction and Coulomb terms due to the S lattice ion can be accurately represented by means of a model potential of the form discussed by Bonifacic and Huzinaga (*35*)

$$V^S_{\text{MP}}(r) = -Z^S r^{-1} \left(1 + \sum_{k=1}^{N} A(k,S)\, r^{n(k,S)} \exp[-\alpha(k,S) r]\right) \quad (26)$$

where $A(k,S)$, $n(k,S)$, and $\alpha(k,S)$ are fitting parameters. In Table VII we collect our best values for these parameters.

A. The Hartree Lattice Model

The Hartree model appears when the electronic structure of the lattice ions is described by a Hartree product instead of an antisymmetric wave function. In consequence, the cluster–lattice exchange inter-

TABLE VIII

RESULTS FROM THE HARTREE LATTICE MODEL (HARTREE) FOR NaF_6^{5-} (FIRST ROWS) AND FNa_6^{5+} (SECOND ROWS)

R(Å)	2.00	2.15	2.25	2.35	2.45	2.60
$\langle V_{eff} \rangle$	−5.78208	−5.24111	−4.94859	−4.69712	−4.47644	−4.19350
	−5.59971	−5.11044	−4.84049	−4.60623	−4.39952	−4.13342
$\langle \Sigma P^S \rangle$	2.55792	1.50947	1.05225	0.73159	0.50722	0.29406
	0.29802	0.16907	0.11299	0.07564	0.05069	0.02814
$\frac{1}{2}E_{int}$	−1.61208	−1.86582	−1.94817	−1.98277	−1.98461	−1.94972
	−2.65085	−2.47069	−2.36375	−2.26530	−2.17442	−2.05264
E_{eff} + 757	−1.79923	−2.85566	−3.25870	−3.50308	−3.63673	−3.70237
E_{eff} + 1069	−3.91000	−3.72138	−3.59278	−3.46441	−3.33903	−3.16292
E_{net} + 757	1.42493	0.87598	0.63764	0.46245	0.33249	0.19707
E_{net} + 1069	1.39169	1.21999	1.13472	1.06619	1.00980	0.94236
E_{add} + 757	−0.18715	−0.98984	−1.31053	−1.52032	−1.65212	−1.75265
E_{add} + 1069	−1.25916	−1.25070	−1.22903	−1.19911	−1.16462	−1.11028
E_{cryst} + 261	−0.06376	−0.17722	−0.21994	−0.24563	−0.25953	−0.26613

action is neglected. Results of this model for the NaF_6^{5-} and the FNa_6^{5+} clusters at several interionic distances can be seen in Table VIII.

In this table we see that the expectation values of the effective potential are very similar for the NaF_6^{5-} and FNa_6^{5+} systems, particularly at larger distances. This energy becomes increasingly attractive when the interionic distance decreases.

The lattice-projection contribution makes a large difference between the two clusters and it is mainly responsible for the differences in the interaction energy.The projection energy is larger in the NaF_6^{5-} cluster because the fluoride density is more extended than the sodium density.

The net energies of the Hartree model, E_{net}^{H}, are repulsive. In NaF_6^{5-} the $E_{net}^{H}(R)$ function is particularly steep, due again to the more diffuse electron distribution of the fluoride ions. These energies can be compared with the corresponding values at the cluster–*in vacuo* level, E_{net}^{0}. The latter are the entries in Table II. We can see that $\Delta E_{net} = E_{net}^{H} - E_{net}^{0} > 0$ for these two clusters. This is so because in the Hartree calculation we introduce the effective repulsions associated to the renormalization and the core projection, plus the possible deformation of the cluster wave function induced by the lattice operators appearing in the Fock operator. In FNa_6^{5+}, the compact density of the Na^+ ligands makes the renormalization correction extremely small and we find values of ΔE_{net} ranging from 0.03 hartree at 2.15 Å to 0.005 at 2.60 Å. In NaF_6^{5-} the renormalization is important and we find $\Delta E_{net} = 0.5$ hartree at 2.15 Å and 0.087 at 2.60 Å.

The additive energy is rather different for these two clusters (see Fig. 6.). In FNa_6^{5+} it increases slowly with R but the opposite is true for the NaF_6^{5-}. As in the single-ion clusters considered in the PI model, the anionic additive energy behaves as a strongly repulsive interaction, their cationic counterpart being slightly attractive. As a result, we find a crystal energy slightly repulsive, from 2.0 to 2.6 Å.

It may be interesting to compute the lattice energy E_{latt} at 2.35 Å, our closest value to the observed R_e. The energy of the infinitely separated ions is obtained by feeding Eq. (7) with the numbers in the last row of

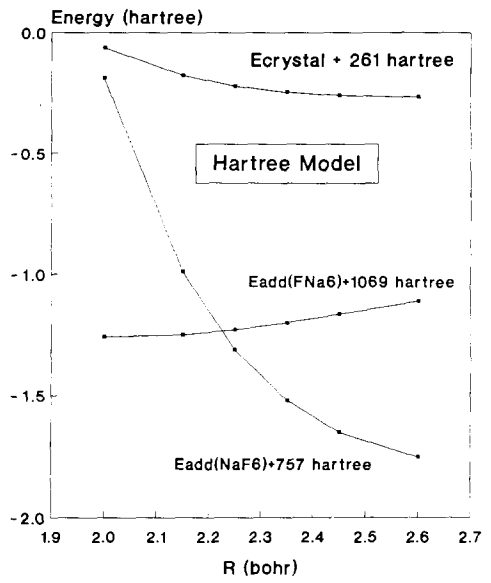

FIG. 6. Additive energy (hartree) of the NaF_6^{5-} and the FNa_6^{5+} clusters, and crystal energy of the NaF, according to the Hartree model.

Table II. We find -260.94537 hartree. From Table VIII we get $E_{\text{crystal}} = -261.24563$ hartree. The lattice energy is then, at this distance, 0.30026 hartree = 188 kcal/mole. This number is nearly 30 kcal/mole too short with respect to the experimental value.

In conclusion, this sophisticated lattice model predicts an unstable crystal and gives a vertical lattice energy in error by 30 kcal/mole. This calculation shows the sensibility of these predictions to the details of the cluster–lattice interaction.

B. The Model Potential Lattice Model

The MP lattice model is the Hartree model enlarged with the nonlocal exchange term in Eq. (23). This quantum lattice contribution works as an effective attraction energy in the cluster space, more intense for shorter cluster sizes. This action of the exchange terms was already observed by Löwdin (*36*). The MP results appear in Table IX.

The expectation value of the effective potential is now more negative, particularly at shorter distances. This effect is larger in the NaF_6^{5-} cluster due to the more extended electron density of the ligands. The modification of the cluster Fock operator due to the lattice exchange term does not produce observable changes in the cluster wave function. This can be seen in the expectation values of the lattice projection operator as well as in the net energy. Both quantities in Table IX coincide with their corresponding entries in Table VIII. Due to this, the modifications in the interaction energy produced by the exchange interactions are those appearing in the effective potential.

These modifications are propagated into the additive energies that become more negative for the two clusters, particularly at smaller distances (Fig. 7). The crystal energy gives a bound crystal, with an electronic energy curve very symmetrical around the minimum at $R_e = 2.247$ Å. At this geometry we find a crystal energy of -261.31467 hartree ($E_\infty = -260.94537$ har-

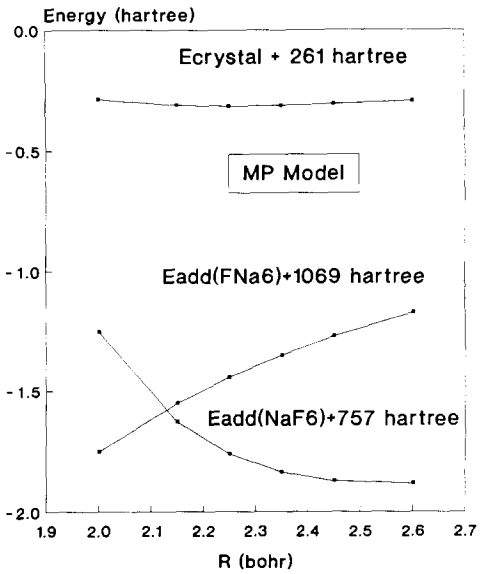

FIG. 7. Additive energy of the NaF_6^{5-} and the FNa_6^{5+} clusters, and crystal energy of the NaF, according to the Model Potential lattice model.

TABLE IX

RESULTS FROM THE MODEL POTENTIAL LATTICE MODEL (HARTREE) FOR NaF_6^{5-} (FIRST ROWS) AND FNa_6^{5+} (SECOND ROWS)

R(Å)	2.00	2.15	2.25	2.35	2.45	2.60
$\langle V_{eff} \rangle$	−7.91433	−6.51781	−5.84609	−5.32582	−4.91535	−4.45036
	−6.58269	−5.71226	−5.26852	−4.90861	−4.61171	−4.25787
$\langle \Sigma P^S \rangle$	2.55792	1.50947	1.05225	0.73159	0.50722	0.29406
	0.29802	0.16907	0.11299	0.07564	0.05069	0.02814
	−2.67821	−2.50417	−2.39692	−2.29712	−2.20407	−2.07815
$\frac{1}{2}E_{int}$	−3.14234	−2.77160	−2.57777	−2.41649	−2.28051	−2.11487
E_{eff} + 757	−3.93149	−4.13236	−4.15619	−4.13179	−4.07564	−3.95923
E_{eff} + 1069	−4.89297	−4.32320	−4.02081	−3.76679	−3.55122	−3.28736
E_{net} + 757	1.42492	0.87598	0.63764	0.46245	0.33249	0.19707
E_{net} + 1069	1.39170	1.22000	1.13472	1.06619	1.00980	0.94236
E_{add} + 757	−1.25328	−1.62819	−1.75927	−1.83468	−1.87158	−1.88108
E_{add} + 1069	−1.75064	−1.55161	−1.44305	−1.35031	−1.27071	−1.17250
E_{cryst} + 261	−0.28628	−0.31140	−0.31462	−0.31214	−0.30604	−0.29337

tree, Table II) and a lattice energy of 0.36930 hartree = 231.7 kcal/mole. This number deviates by about 5% from the experimental range. From the computed $E_{crystal}(R)$ curve we obtain a bulk modulus of 59.4 GPa at R_e, in good agreement with the observed 51.4 GPa (*37*). It is necessary to recall, however, the high sensitivity of the computed bulk modulus against changes in the fitting expression used to represent the values of $E_{crystal}$.

In conclusion, adding the lattice exchange term into the Hartree model does not have any appreciable effect in the cluster wave function and the cluster net energy. As a consequence, the lattice projection remains also unaffected. However, the exchange term makes more negative the cluster–lattice interaction and this effect is enough, in this case, to produce a stable crystal. We see here a clear example of the significance of the approximations adopted for the cluster–lattice interaction.

Having a bound crystal, we can study the behavior of the system under high pressure. We compute the Gibbs free energy isobars of Eq. (20) from 0 to 50 GPa. From a plot like that in Fig. 3 we obtain the minimum values R_0 and $G(p,R_0)$ at each selected pressure p. This gives the cell volume $V(p) = 2R_0^3$ and the p–V behavior of the crystal. This behavior has been plotted in Fig. 4, where we can see the good agreement between the experimental data reported by Drickamer and co-workers (*30, 38*) and the MP prediction for the fcc phase. The pressure dependence of the bulk modulus is computed with Eq. (27),

$$B(p) = (18R)^{-1}(\partial^2 E_{crystal}(R)/\partial R^2) - (9R^2)^{-1})\partial E_{crystal}(R)/\partial R), \quad (27)$$

where the partial derivatives are computed for each pressure at the corresponding R_0. The values of $G(p,R_0)$ give also (when subtracted from E_∞) the lattice energy at the pressure p. Our numerical results are collected in Table X.

The bulk modulus varies linearly with pressure. The MP prediction is B(GPA) = 59.43 + 4.93 p(GPa). The Gibbs free energy at the minimum of each isobar and the crystal energy are plotted in Fig. 8 for the range of pressures analyzed here. These two curves coincide at zero pressure. Since these numbers correspond to 0 K, the crystal energy coincides with the Helmholtz

TABLE X

PRESSURE EFFECTS FOR THE fcc PHASE OF NaF ACCORDING TO THE MODEL POTENTIAL LATTICE MODEL

p(GPa)	R_e(Å)	V(Å^3)	V/V_0	B(GPa)	E_{latt}(kcal/mole)
0	2.247	22.69	1.000	59.43	231.7
5	2.195	21.15	0.932	83.98	216.0
10	2.157	20.07	0.885	109.2	201.2
20	2.103	18.61	0.820	157.8	173.4
25	2.083	18.07	0.796	181.6	160.2
30	2.066	17.63	0.777	203.5	147.1
40	2.032	16.77	0.739	255.4	122.3

function of the crystal and its slope in Fig. 8 is the negative of the applied pressure. The second derivative is positive all along the range and consequently we have $(\partial p/\partial V)_T < 0$ up to 50 GPa. In this figure we also see the steep increase of the pV energy term (the difference between the two curves) with increasing pressure.

According to an approximation advanced by Löwdin (*36*), the repulsion energy in NaF and other highly ionic compounds, E_{rep}, should depend essentially upon the number of first neighbors and should be the same for the fcc and bcc structures. The only difference would come from the many-body energy terms that are proportional to the Madelung constant. Since the Madelung constant for these two structures is very similar, this difference should be really small. Assuming this approximation, we can write the crystal energy in the form

$$E^{fcc}_{crystal}(R) = E_\infty - A^{fcc}_M/R + n\,E_{rep}(R), \quad (28)$$

where A_M is the Madelung constant and n the number of first neighbors. Equation (28) gives us the possibility of estimating the crystal energy of the bcc phase of the NaF without performing new cluster-in-the-lattice calculations. From the fcc energy we obtain:

$$E^{bcc}_{crystal}(R) = E_\infty - A^{bcc}_M/R + 4(E^{fcc}_{crystal}(R) - E_\infty + A^{fcc}/R)/3. \quad (29)$$

In Table XI we show the values of the Löwdin repulsion energy and the corresponding crystal energy for the bcc phase. This repulsion energy is noticeably different from the nonclassical energy in Eq. (11) since we deal here with a larger number of interionic interactions. The Löwdin E_{rep} can be approximated by means of the exponential E_{rep}(hartree) = 183.25708 exp(−4.53486 R(Å)) only with qualitative accuracy, since

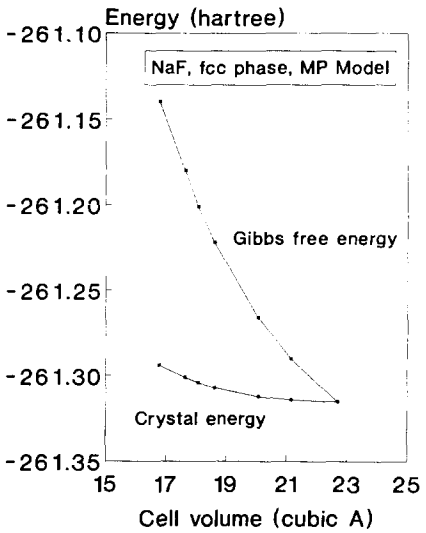

FIG. 8. Pressure effects on the crystal energy and Gibbs free energy of NaF according to the Model Potential lattice model.

TABLE XI

BINDING ENERGIES (HARTREE) FOR THE fcc PHASE (MODEL POTENTIAL LATTICE MODEL) AND bcc PHASE (LÖWDIN APPROXIMATION, EQS. (28) AND (29))

	2.00	2.15	2.25	2.35	2.45	2.60
$E_{fcc} - E_{\infty}$	−0.34090	−0.36602	−0.36924	−0.36676	−0.36066	−0.34799
$E_{bcc} - E_{\infty}$	−0.30440	−0.34824	−0.35883	−0.36124	−0.35831	−0.34844
E_{rep}	0.02024	0.01074	0.00699	0.00447	0.00280	0.00132

this formula gives deviations of about 5% (see Fig. 9).

The crystal energy of the bcc lattice gives the Gibbs function

$$G^{bcc}(R,p) = E^{bcc}_{crystal}(R) + 8(3)^{1/2}R^3p/9. \tag{30}$$

From this free energy we have computed the results in Table XII for the bcc phase. In agreement with the Löwdin observation (*36*), the bcc phase has a larger equilibrium distance but a shorter cell volume than the fcc phase. Our numbers show a bcc volume about 87% of the fcc volume, at zero pressure. Cohen and Gordon (*18*) found a 92% value. The bulk modulus for the bcc phase is also linear in the pressure, with a somewhat larger intercept and smaller slope than the fcc function. The fcc and bcc $B(p)$ functions cross each other near 20 GPa.

Comparing the fcc lattice energy in Table X with the bcc energy in Table XII we see that a crossing occurs around 15–20 GPa. Cohen and Gordon predicted a transition pressure of 32 GPa and other semiempirical calculations (*39*) give transition pressures near 20 GPa. Other calculations like those by Yamashita and Asano (*40*) and Bose, Ghosh, and Basu (*41*) also predict a fcc–bcc transition below 50 GPa. As noted before, such transition has been detected by Yagi *et al.* (*31*) at 27 GPa. However, the p–V data by Drickamer and co-workers (*30, 38*) do not support such transition, as can be seen in Fig. 4, where the MP results for the p–V behavior of the bcc structure have also been plotted. The discrepancy, as far as our calculation is concerned, may perfectly be due to the different quality of the calculation for fcc and bcc phases. Due to this, the results for the bcc phase presented here should be viewed as first-order estimates. To maintain the standard of the MP model, we should perform cluster-in-the-lattice calculations on the conjugate cubal NaF_8^{7-} and FNa_8^{7+} units.

The results presented here are a simple example of the potential usefulness of a new theoretical tool: a standard ab initio molecu-

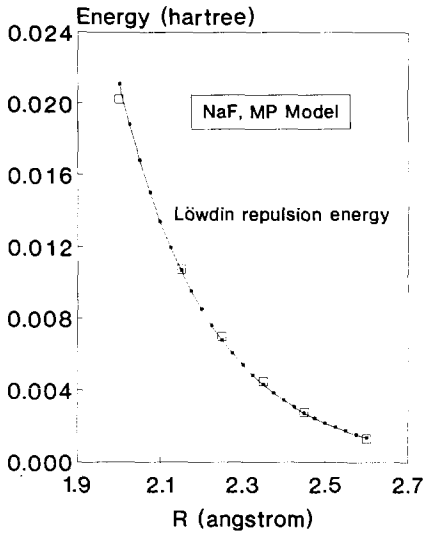

FIG. 9. Exponential approximation to the Löwdin repulsion energy (solid line): E_{rep}(hartree) = 183.25708 exp(−4.53486 R(Å)). Empty squares are the predictions of the Model Potential lattice model.

TABLE XII

PRESSURE EFFECTS FOR THE bcc PHASE ACCORDING TO THE MODEL POTENTIAL LATTICE MODEL AND THE LÖWDIN APPROXIMATION

p(GPa)	R_e(Å)	V(Å^3)	V/V_0^{fcc}	B(GPa)	E_{latt}(kcal/mole)
0	2.338	132.86	0.868	72.8	226.7
5	2.292	125.08	0.817	92.2	213.0
10	2.255	119.11	0.778	113.1	200.0
20	2.199	110.52	0.722	157.8	175.5
25	2.178	107.28	0.701	180.9	163.7
30	2.159	104.57	0.683	203.6	152.6
40	2.127	100.02	0.653	249.9	130.8

lar package, interfaced with a set of cluster–lattice interaction routines, able to keep track of all different interaction components of the total energy. The PI model is the first, yet limited, full implementation of such a tool with a cluster defined as a single ion. The cluster calculations presented here have been performed with the methodology developed by Richardson's group. They contain multiple approximations and cannot easily be extended to large, realistic SCF spaces. Even so, this type of cluster calculation has been very useful in the detailed study of many difficult problems of the electronic structure of ionic solids containing open-shell, transition metal impurities. The present analysis reveal that they are also useful for describing the electronic structure of simple ionic crystal. We believe that the results reported in this paper might attract the attention of individuals developing molecular packages and interested in the electronic structure of solids and thus lead them to include in their programs the necessary elements to exploit the great analytical advantages of the TES.

Acknowledgments

The authors are indebted to M. Flórez, E. Francisco, and A. Martín Pendás for stimulating conversations. Financial support from the Dirección General de Investigación Científica y Técnica (DGICYT) del Ministerio de Educación y Ciencia (Spain), under Project No. PB86-0240, is gratefully acknowledged.

References

1. J. M. VAIL AND R. PANDEY, *Mater. Res. Soc. Symp. Proc.* **63,** 247 (1985).
2. J. M. VAIL, R. PANDEY, AND A. H. HARKER, *Cryst. Latt. Def. Amorph. Mater.* **15,** 13 (1987).
3. R. PANDEY AND J. M. VAIL, *J. Phys.: Condens. Matter* **1,** 2801 (1989).
4. N. E. BRENER AND J. CALLAWAY, *Phys. Rev. B* **35,** 4001 (1987).
5. G. J. M. JANSSEN AND W. C. NIEUWPOORT, *Phys. Rev. B* **38,** 3449 (1988).
6. J. W. RICHARDSON AND G. J. M. JANSSEN, *Phys. Rev. B* **39,** 4958 (1989).
7. S. Y. SHASHKIN AND W. A. GODDARD III, *Phys. Rev. B* **33,** 1353 (1986).
8. N. W. WINTER, R. M. PITZER, AND D. K. TEMPLE, *J. Chem. Phys.* **87,** 2945 (1987).
9. Z. BARANDIARÁN AND L. SEIJO, *J. Chem. Phys.* **89,** 5739 (1988).
10. T. A. GREEN AND D. R. JENNISON, *Phys. Rev. B* **36,** 6112 (1987).
11. V. LUAÑA AND L. PUEYO, *Phys. Rev. B* **39,** 11093 (1989).
12. V. LUAÑA AND L. PUEYO, *J. Mol. Struct. (Theochem.)* **15,** 45 (1988).
13. V. LUAÑA AND L. PUEYO, *Phys. Rev. B*, **41,** 3800 (1990).
14. E. MIYOSHI AND H. KASHIWAGI, *Int. J. Quantum Chem.* **24,** 85 (1983).
15. V. LUAÑA, M. BERMEJO, M. FLÓREZ, J. M. RECIO, AND L. PUEYO, *J. Chem. Phys.* **90,** 6409 (1989).
16. S. HUZINAGA, L. SEIJO, Z. BARANDIARÁN, AND M. KLOBUKOWSKI, *J. Chem. Phys.* **86,** 2132 (1987).
17. J. W. RICHARDSON, T. F. SOULES, D. M. VAUGHT, AND R. R. POWELL, *Phys. Rev. B* **4,** 1721 (1971).

18. A. J. COHEN AND R. G. GORDON, *Phys. Rev. B* **12,** 3228 (1975).

19. J. YAMASHITA AND S. ASANO, *J. Phys. Soc. Japan* **53,** 3112 (1984).

20. J. M. RECIO, V. LUAÑA, AND L. PUEYO, *J. Chem. Educ.* **66,** 307 (1989).

21. B. L. KALMAN AND J. W. RICHARDSON, *J. Chem. Phys.* **55,** 4443 (1971).

22. E. FRANCISCO, Ph.D. thesis, Universidad de Oviedo (1988).

23. L. SEIJO, Z. BARANDIARÁN, V. LUAÑA, AND L. PUEYO, *J. Solid State Chem.* **61,** 269 (1986).

24. V. LUAÑA, G. FERNÁNDEZ RODRIGO, E. FRANCISCO, L. PUEYO, AND M. BERMEJO, *J. Solid State Chem.* **66,** 263 (1987).

25. E. CLEMENTI AND C. ROETTI, *At. Data Nucl. Data Tables* **14,** 177 (1974).

26. E. FRANCISCO, L. SEIJO, AND L. PUEYO, *Compt. Phys. Commun.* **43,** 269 (1987).

27. L. PUEYO AND J. W. RICHARDSON, *J. Chem. Phys.* **67,** 3583 (1977).

28. M. BERMEJO, V. LUAÑA, J. M. RECIO, AND L. PUEYO, *J. Mol. Struct. (Theochem).* **166,** 235 (1988).

29. R. A. COWLEY, *Proc. R. Soc. Ser. A* **268,** 121 (1962).

30. H. G. DRICKAMER, R. W. LYNCH, R. L. CLENDENEN, AND E. A. PÉREZ-ALBUERNE, *in* "Solid State Physics" (H. Ehrenreich, F. Seitz, and D. Turnbull, Eds.), Vol. 19, p. 135, Academic Press, New York (1965).

31. T. YAGI, T. SUZUKI, AND S. I. AKIMOTO, *J. Phys. Chem. Solids* **44,** 135 (1983).

32. R. W. ROBERTS AND C. S. SMITH, *J. Phys. Chem. Solids* **31,** 619 (1970).

33. S. HART AND P. H. GREENWOOD, *Solid State Commun.* **46,** 161 (1983).

34. S. HART, *Mater. Res. Soc. Symp. Proc.* **22,** 239 (1984).

35. V. BONIFACIC AND S. HUZINAGA, *J. Chem. Phys.* **62,** 1509 (1975).

36. P. O. LÖWDIN, *Adv. Phys.* **5,** 1 (1956).

37. J. T. LEWIS, A. LEHOCZKY, AND C. V. BRISCOE, *Phys. Rev.* **161,** 877 (1967).

38. M. PAGANNONE AND H. G. DRICKAMER, *J. Chem. Phys.* **43,** 2266 (1965).

39. M. BORN AND K. HUANG, "Dynamical Theory of Crystal Lattices," Oxford Univ. Press (Clarendon), London/New York (1954).

40. J. YAMASHITA AND S. ASANO, *J. Phys. Soc. Japan* **52,** 3506 (1983).

41. D. BOSE, A. GHOSH, AND A. N. BASU, *Phys. Rev. B* **29,** 3632 (1984).

42. P. B. GHATE, *Phys. Rev. A* **139,** 1666 (1965).

43. T. C. WADDINGTON, *Adv. Inorg. Chem. Radiochem.* **1,** 157 (1959).